Int. J. Electrochem. Sci., 6 **(2011)** 3140 - 3163

International Journal of
ELECTROCHEMICAL
SCIENCE
www.electrochemsci.org

Some New Thiadiazole Derivatives as Corrosion Inhibitors for 1018 Carbon Steel Dissolution in Sodium Chloride Solution

F. El-Taib Heakal [1,*], *A.S. Fouda* [2], *M.S. Radwan* [3]

[1] Chemistry Department, Faculty of Science, Cairo University, Giza 12613, Egypt
[2] Chemistry Department, Faculty of Science, El-Mansoura University, Egypt
[3] Petrogulf Misr Company, Maadi, Cairo, Egypt
[*]E-mail: fakihaheakal@yahoo.com

Received: 17 May 2011 / *Accepted:* 11 July 2011 / *Published:* 1 August 2011

Three new thiadiazole derivatives (TDADs), namely, (I) N-[4-phenyl-5-(p-tolylimino)-4,5-dihydro-1,3,4-thiadiazole-2-yl] benzamide, (II) 2-acetyl-4-phenyl-5-(p-tolylimino)-4,5-dihydro-1,3,4-thiadiazole, and (III) Ethyl-4-phenyl-5-(p-tolylimino)-4,5-dihydro-1,3,4-thiadiazole-2-carboxylate, have been synthesized and used as additives to protect grade 1018 carbon steel from corrosion in naturally aerated 0.5 M NaCl solution (~ 3% by wt.). The techniques adopted include open circuit potential (OCP), potentiodynamic polarization and electrochemical impedance spectroscopy (EIS) complemented by surface examination via scanning electron microscope (SEM). It was found that the quasi-steady state OCP value shifts positively with increasing TDAD concentration. Polarization technique showed that TDADs (I–III) are anodic-type inhibitors, where the corrosion rate decreases with increasing the inhibitor concentration or decreasing temperature. At any given conditions, the protection efficiency increases in the order III > II > I as confirmed by SEM observation. Impedance parameters (R_t and C_{dl}) indicate the formation of protective films via the adsorption of inhibitor molecules on the metal surface. Thermodynamic parameters of the corrosion and adsorption processes indicate generally that adsorption of these compounds on 1018 carbon steel surface occurs spontaneously through both electrostatic (ionic) and chemisorption (molecular) mechanism following Langmuir adsorption isotherm.

Keywords: Thiadiazole, corrosion protection, carbon steel, thermodynamics, EIS.

1. INTRODUCTION

Because of its hardness and low cost, carbon steel is a metallic constructional material commonly used for the majority of pipelines and vessels in oil production and refinery plants. Carbon atoms has a hardening effect on iron as they fit into the interstitial crystalline lattice sites of the body-centered cubic (bbc) arrangement of the iron atoms and thus reduces the mobility of dislocations, which

in turn cause some of the iron bbc lattice cells to distort. Crude oil often contains in addition to CO_2 and H_2S gases significant concentration of chloride ions, which are usually recognized as the main cause of carbon steel pitting corrosion due to their aggressive nature, leading to passive layer breakdown [1,2]. The aggressiveness of chloride ion is due to its small size, high diffusivity and strong acidic anionic nature [3]. Many studies have been made on the corrosion behavior of carbon steel in carbonated-chloride brines [1,4]. Chloride induced corrosion can be generally mitigated by using inhibitors, which are chemical substances that retard the rate of corrosion of metal when added in minute quantity. Heterocyclic compounds having π-bonds and containing one or more polar groups with N, O and S atoms generally give rise to satisfying inhibition efficiency for steel corrosion in acidic media [5].

Various thiadiazole compounds have been synthesized and evaluated as corrosion inhibitors for mild steel in acidic chloride and sulfate solutions [6-12]. The inhibition efficiency is generally affected by the chemical changes occurring to the inhibitor, by the nature and surface charge of metal and by the type of the aggressive electrolytic medium, and is ascribed to the effect of functional groups connected with aromatic rings. The primary step in the mechanism of inhibition by these organic compounds is generally accepted as the adsorption of the inhibiting species on the metal surface [13,14]. The polar function is frequently regarded as the reaction center for the adsorption process establishment, and the adsorption bond strength is determined by the electron density and polarizability of the functional group [15]. To be effective, an inhibitor must first displace water molecules from the metal surface, and then interact with anodic and/or cathodic corrosion reaction and prevent transportation of water and corrosive-active species to the surface [16].

Despite a relatively large number of studies on the corrosion inhibition of carbon steel in acidic media [6-12,16], data in neutral chloride solution are meager. Therefore, it seems interesting to investigate the role of some newly prepared thiadiazole derivatives as corrosion inhibitor for grade 1018 carbon steel in 0.5 M NaCl solution (~3 wt.%), and to explore the influence of those substances on the pitting corrosion potential of the steel in neutral chloride medium. The study utilized electrochemical techniques and SEM observations. The tested thiadiazole derivatives are considered as non-cytotoxic substances, i.e. they are eco-friendly compounds. The environment-friendly property makes them favorable to be used in practice, replacing some toxic organic inhibitors in agreement with the new environmental restrictions need to use green ones [17]. It was also our goal to correlate the obtained protection efficiencies with some electronic properties of the tested thiadiazole molecules.

2. EXPERIMENTAL

2. 1. Chemicals and materials

The test solution was prepared from a stock solution of 4.0 M NaCl by dilution to 0.5 M (~3 wt.%) with bi-distilled water and used as corrosive medium. All experiments were performed at 298 ± 1 K unless otherwise stated, with 1018 carbon steel material having chemical composition in wt.% of: 0.200 C, 0.350 Mn, 0.024 P, 0.003 Si and the remainder is iron. The three TDADs (I-III) used in the present study were prepared according to the literature [18] and checked after preparation by melting

point, chemical analysis and nuclear magnetic resonance; their chemical structures and molecular weights are shown in Fig. 1. Stock solutions of 0.001 M from each derivative were prepared by dissolving the appropriate weighted amount of the compound in absolute acetone. In all test solutions the acetone content was kept at a constant value of 1.1% by volume. The inhibitors were used over the concentration range 1 – 11 μM. After each addition the solution appeared always clear, indicating complete solubility of the TDADs in neutral chloride medium.

2.2. Potentiodynamic polarization

Potentiodynamic polarization experiments were carried out in a typical three-electrode glass cell with a capacity of 100 ml fitted with a large platinum sheet of size 20mm × 10mm × 2mm as a counter electrode and a saturated calomel (SCE) reference electrode (E_{SCE} = 0.241 V vs. SHE). The working electrode was in the form of a disc fixed in a suitable glass jacket with an epoxy resin leaving a constant exposed surface area of 0.12 cm^2 to contact the test solution. The surface of the test electrode was mechanically abraded by emery papers of 400 up to 1000 grit to ensure the same surface roughness. A time interval of about 30 min from immersion was given for the test electrode to attain steady state conditions and its open circuit potential (E_{oc}) was monitored with time. Both cathodic and anodic potentiodynamic polarization curves were recorded over the potential domain 500 mV(SCE) ± E_{oc} with a scan rate of 1.0 mV s^{-1}, using Gamry instruments (version 3.20) Potentiostat/Galvanostat/ZRA (Gamry Inc., USA). This system was interfaced to a personal computer to control the experiments and the data were analyzed using Gamry framework/analysis software. The protection efficiency (η_i) was calculated using the following equation:

$$\eta_i = \frac{i_{corr} - i'_{corr}}{i_{corr}} \times 100 \quad (1)$$

where i_{corr} and i'_{corr} are the corrosion current densities in the absence and presence of the inhibitor, respectively.

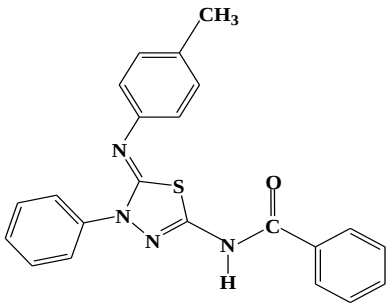

(I) N-[4-phenyl-5-(p-tolylimino)-4,5-dihydro-1,3,4-thiadiazole-2-yl] benzamide. Molecular weight = 385

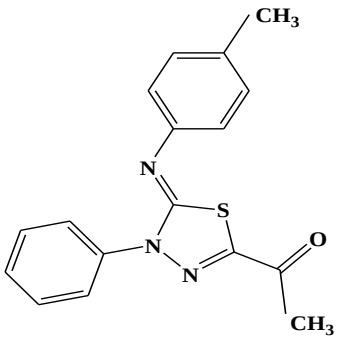

(II) 2-acetyl-4-phenyl-5-(p-tolylimino)-4,5-dihydro-1,3,4-thiadiazole. Molecular weight = 309

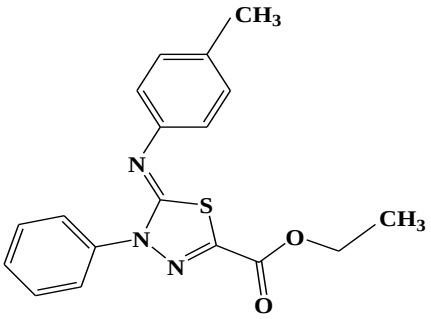

(III) Ethyl-4-phenyl-5-(p-tolylimino)-4,5-dihydro-1,3,4-thiadiazole-2-carboxylate. Molecular weight = 339

Figure 1. Chemical structure and molecular weight of the investigated thiadiazole derivatives.

2.3. Electrochemical impedance spectroscopy (EIS)

EIS experiments were conducted at E_{oc} value over a frequency range (100 kHz to 1 Hz) with a low amplitude of 10 mV for the voltage excitation signal using Potentiostat/Galvanostat/ZRA analyser (Gamry PCI300/4). A personal computer with EIS300 software and Echem Analyst 5.21 was used for fitting the spectra and calculating the equivalent circuit parameters. Nyquist and Bode plots were obtained from the results of the EIS experimental data. Values of the charge transfer resistance (R_t) were obtained from these plots by determining the difference in the values of impedance at low and high frequencies, as suggested by Heakal and Haruyama [19]. The values of the double layer capacitance (C_{dl}) were calculated from the frequency at which the impedance imaginary component ($-Z''$) was maximum, using the following equation [20]:

$$C_{dl} = 1/2\pi\, f_{(-Z''max)} R_t \qquad (2)$$

The percentage protection from impedance results (η_{Rt}) was calculated using the equation:

$$\eta_{Rt} = \frac{(1/R_t) - (1/R'_t)}{(1/R_t)} \times 100 \qquad (3)$$

where R_t and R'_t are the charge transfer resistance values in the absence and presence of inhibitors, respectively.

2.4. Scanning Electron Microscopy (SEM)

Carbon steel samples was treated as mentioned in Section 2.2, immersed in 0.5 M NaCl solution in the absence and presence of 11 μM of inhibitors (I–III) for 2 h at E_{oc} then SEM micrographs were collected using the JEOL JXA-840A electron probe microanalyzer.

3. RESULTS AND DISCUSSION

3.1. Open-circuit potential measurements

Prior to the commencement of each polarization experiment the open-circuit potential (E_{oc}) of 1018 carbon steel electrode in 0.5 M NaCl solutions free or containing various concentrations from TDAD I, II or III was monitored with time for 30 min at 298 K to reach its steady state potential under stabilized conditions. The transients obtained for derivative (III) as an example, are shown in Figure 2. In all cases, E_{oc} drifts with time in the active direction and tends to stabilize within 6 min.

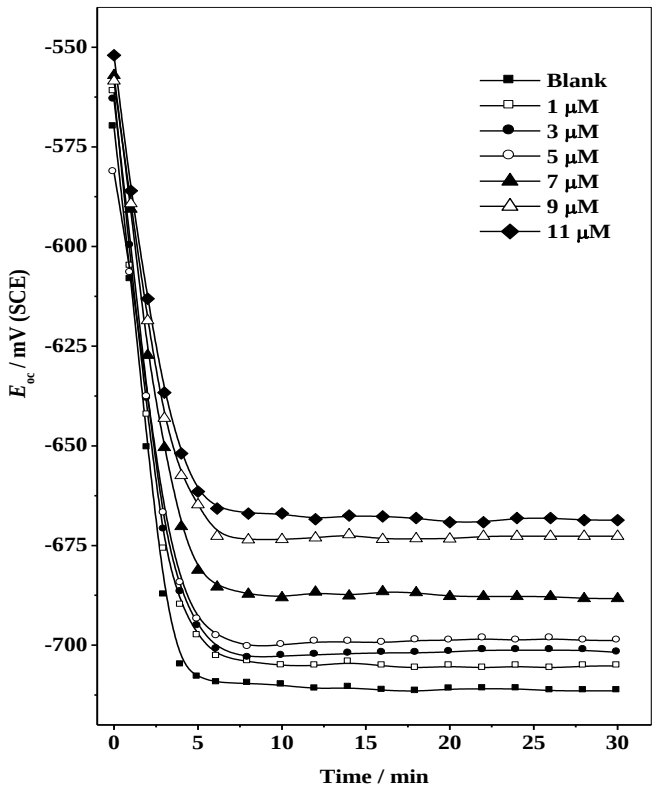

Figure 2. Variation of the open circuit potential (E_{oc}) with time for 1018 carbon steel in 0.5 M NaCl solution in the absence and presence of different concentrations of TDAD (III) at 298 K.

The negative shift of potential with time is related to active dissolution of carbon steel in sodium chloride solution [21]. The stabilized potential value was found to be always more negative than the immersion potential value (E_{oc} at t = 0), suggesting that the native oxide film on the sample surface is unstable under the prevailing conditions and suffers from thining before achieving a steady condition [22]. Generally, the steady E_{oc} value, which corresponds to the free corrosion potential of the bare metal [23], was found to move significantly in the noble direction as the inhibitor concentration increases. This implies that under these conditions TDADs (I–III) function as anodic-type inhibitors, and their ability to mitigate carbon steel corrosion are more enhanced at higher additions. The progressive positive shift can be attributed to possible adsorption of thiadiazole molecules on the active anodic sites and/or the deposition of corrosion products on the electrode surface.

3.2. Potentiodynamic polarization method

3.2.1. Electrochemical corrosion

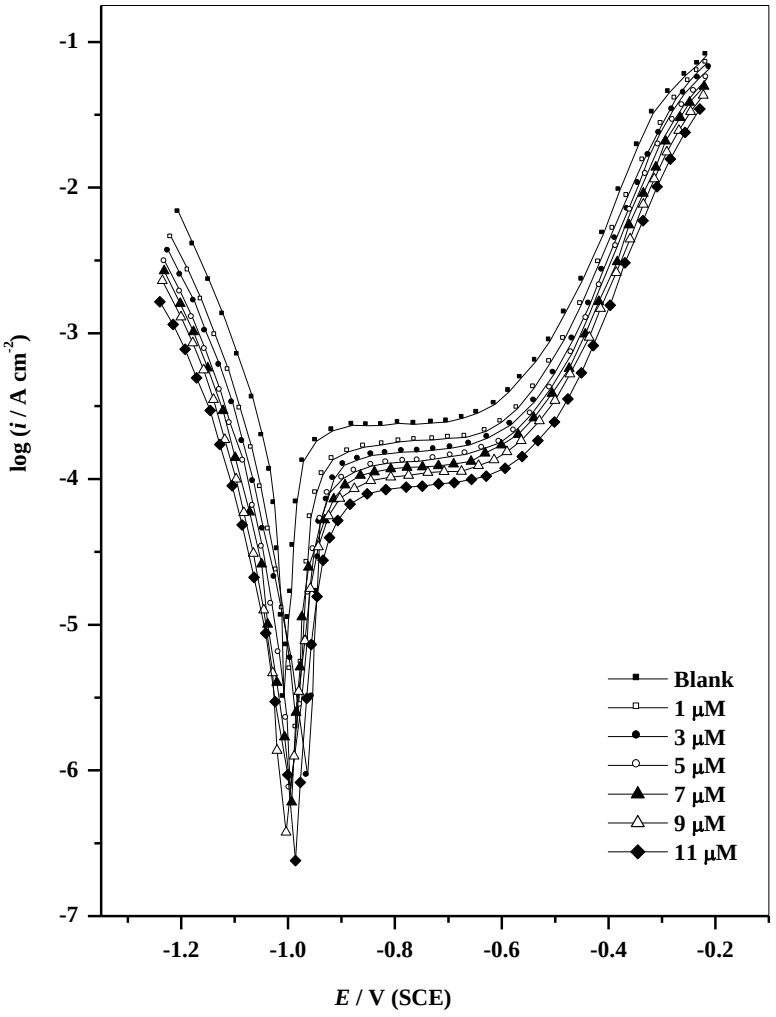

Figure 3. Potentiodynamic cathodic and anodic polarization scans for 1018 carbon steel in 0.5 M NaCl solution in the absence and presence of different concentrations of TDAD (III) at 298 K.

The electrochemical corrosion characteristics of carbon steel in 0.5 M NaCl solution free or containing various concentrations from each inhibitor I, II or III were investigated potentiodynamically at 298 K by recording the cathodic and anodic curves. The potential was scanned automatically from –1.20 to –0.20 V vs. SCE at a rate of 1.0 mV s^{-1}, which allows the quasi-stationary state measurements. Generally, all scans exhibit similar behavior over the potential domain examined, indicating that similar cathodic as well as anodic reactions take place on the metal (cf. Fig. 3). However, in the anodic range from the corrosion potential, the current density starts to increase very steeply due to active metal dissolution reaction, then stabilizes over a passivation zone extending to ~300 mV before it starts again to increase faster due to breakdown of the passive film and pit initiation.

The obtained results enable the determination of various electrochemical corrosion parameters of carbon steel as a function of the inhibitor concentration using the software for *i*/*E* analysis [24]. The corrosion current density (i_{corr}) was determined [25] by extrapolating the cathodic Tafel region back to E_{oc} (i.e. potential of zero current in the potentiodynamic curves or E_{corr}), and all estimated values are listed in Table 1 together with the polarization resistance (R_p), corrosion rate (*CR*) and the protection efficiency (η_i) as a function of each TDAD concentration.

Table 1. Potentiodynamic polarization parameters for the corrosion of 1018 carbon steel in 0.5 M NaCl solution in the absence and presence of different concentrations of compounds (I–III) at 298 K

Inhibitor	Conc. (μM)	$-E_{oc}$ mV(SCE)	$-E_{corr}$ mV(SCE)	i_{corr} (μA cm^{-2})	$-\beta_c$ (mV dec^{-1})	β_a (mV dec^{-1})	R_p (kΩ cm^2)	*CR* (mm y^{-1})	θ	η_i%
Blank	0	712	1008	77	101	550	0.48	0.90	-----	-----
I	1	710	1001	68	101	535	0.51	0.79	0.12	12
	3	707	999	55	99	525	0.55	0.65	0.29	29
	5	704	994	49	95	446	0.56	0.57	0.36	36
	7	701	997	45	99	440	0.62	0.52	0.42	42
	9	696	1001	37	95	433	0.82	0.43	0.52	52
	11	681	982	32	93	432	1.28	0.38	0.58	58
II	1	708	1006	58	94	494	0.57	0.67	0.25	25
	3	706	980	48	91	441	0.70	0.56	0.38	38
	5	705	1004	41	91	413	0.75	0.47	0.47	47
	7	700	1006	34	85	330	0.90	0.40	0.56	56
	9	688	1001	26	75	374	1.60	0.30	0.66	66
	11	680	992	18	71	308	1.74	0.21	0.77	77
III	1	705	998	55	93	411	0.60	0.64	0.29	29
	3	702	990	46	87	399	0.68	0.53	0.40	40
	5	699	993	28	86	387	0.97	0.33	0.64	64
	7	688	1006	26	84	375	1.32	0.31	0.66	66
	9	672	1000	19	85	366	1.36	0.22	0.75	75
	11	668	978	16	70	346	3.85	0.19	0.79	79

In pure chloride solution i_{corr} value of carbon steel sample is 77 μA cm^{-2}; this value gradually decreases on adding increasing concentration from each derivative. In all cases, the increase in inhibitor concentration from 1 μM to 11 μM is accompanied by a decrease in i_{corr} value and, a subsequent increase in η_i% value. For example, the inhibition efficiency increases from 28% to 79% for the most efficient TDAD (III). These results lead to the conclusion that the three compounds under investigation protect quite well carbon steel from degradation in the aggressive chloride medium. The results show also that increasing inhibitor concentration shifts progressively the corrosion potential (E_{corr}) towards less negative values with respect to the blank, indicating that those compounds can inhibit metal dissolution by blocking the active anodic sites on the steel surface.

The cathodic Tafel slope (β_c) remains constant, while the anodic Tafel slope (β_a) is higher than β_c and slightly decreases as the concentration of TDAD increases, indicating no change in the mechanism of its inhibition. The fact that values of β_a are higher than β_c suggests that the three TDADs are all function via anodic-type mechanism. The higher values of the anodic Tafel slope can be attributed to surface kinetic process rather than a diffusion-controlled one [26], where the inhibitor molecules are adsorbed via their polycentric adsorption sites on to the steel surface forming a protective layer. Meanwhile, the constancy of the cathodic Tafel slope indicates that oxygen reduction reaction ($O_2 + 2H_2O = 4OH^-$), which is the main cathodic process here, is under activation control and that addition of TDADs does not modify its mechanism. This result suggests that the inhibition mode of the tested TDADs is by simple blockage of the surface via adsorption. The slight decrease in β_a value with inhibitor concentration is likely a result of an increase in the number of adsorbed organic molecules on the steel, which impede more the diffusion of ions to or from the electrode surface as the degree of surface coverage (θ) increases [27], and that the inhibition mechanism of TDAD molecules in neutral chloride solution is predominantly under anodic control.

Furthermore, the results in Table 1 demonstrate clearly that both i_{corr} and *CR* decrease, while the polarization resistance (R_p) increases with addition of inhibitors indicating the inhibatory effect of TDADs on the carbon steel corrosion. Generally, for a given inhibitor type, R_p value in neutral solution is greater than its value in acidic one, meaning that corrosion rate of carbon steel is more enhanced in acidic media, and that the protective adsorbed layer on the alloy surface is more stable in the neutral solution [28]. This is in agreement with the present results as R_p value calculated in neutral chloride solution was found to be much higher than the previous value calculated in acidic media under comparable conditions [16]. Based on the values of η_i% calculated as a function of inhibitor concentration, which are listed in Table 1, the order of the protection efficiency for the three investigated TDADs remains unchanged, being III > II > I at any given conditions.

3.2.2. Adsorption isotherm

The mechanism of corrosion protection may be explained on the basis of adsorption behavior [29]. Thus, to describe the adsorption performance of the tested TDADs (I–III) on carbon steel attempts were made to apply the effect of inhibitor concentration on the degree of surface coverage (θ) obtained

from polarization measurements to the most frequently used adsorption isotherms: Langmuir, Temkin and Frumkin. By far, the data were best fitted with Langmuir equation, which can be expressed as:

$$C/\theta = 1/K_{ads} + C \quad (4)$$

where K_{ads} is the equilibrium constant of the adsorption process. Therefore, plotting C/θ against the inhibitor concentration (C) for the three tested compounds (Fig. 4) should give linear relationship with a slope of unity and intercept of ($1/K_{ads}$), indicating the validity of Langmiur isotherm and the absence of any attraction or repulsion forces between the adsorbed molecules. It is also known that the constant K_{ads} is related to the standard free energy of adsorption (ΔG^{o}_{ads}) by the following equation:

$$K_{ads} = 1/55.5 \exp(-\Delta G^{o}_{ads}/RT) \quad (5)$$

where 55.5 is the molar concentration of water in the solution, R is the universal gas constant and T is the absolute temperature.

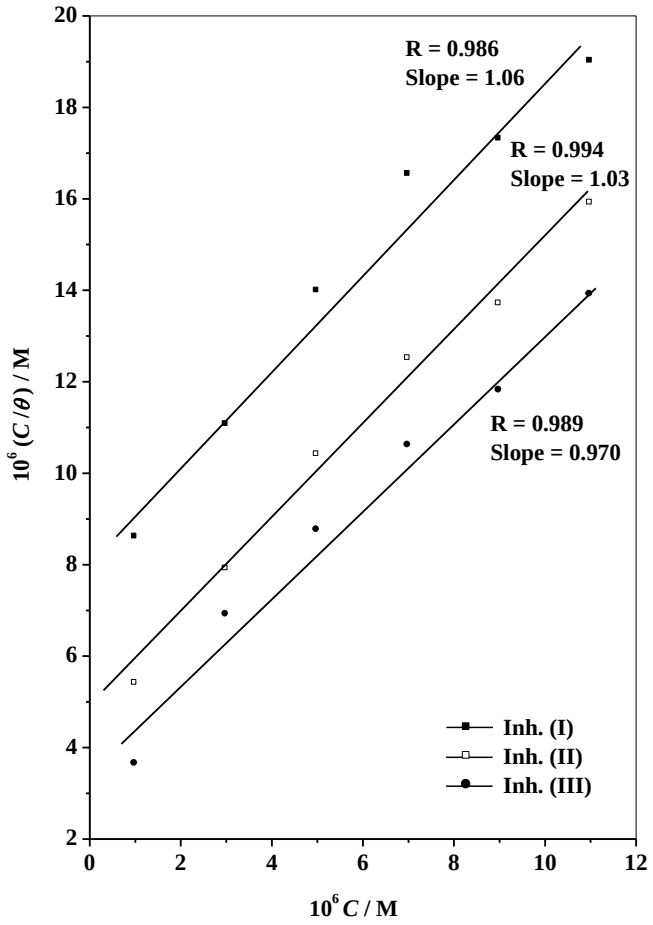

Figure 4. Langmuir adsorption isotherms for 1018 carbon steel in 0.5 M NaCl solution in the presence of different concentrations of TDADs (I–III) at 298 K.

The values of ΔG^{o}_{ads} for inhibitors (I–III) over the temperatures range from 298 to 323 K were calculated and plotted vs. T as shown in Fig. 5, which gives a straight line with a slope equal to the entropy of adsorption (ΔS^{o}_{ads}) and an intercept equal to the enthalpy of adsorption (ΔH^{o}_{ads}) in consistent with the following basic thermodynamic relation [30]:

$$\Delta G^{o}_{ads}=\Delta H^{o}_{ads}-T\Delta S^{o}_{ads} \quad (6)$$

The results shown in Table 2 reveal that for the three TDADs, ΔG^{o}_{ads} is always negative and increases on going from compound (I) to compound (III), indicating that over the studied temperature range these compounds can be adsorbed spontaneously on carbon steel surface forming fairly stable adsorbed layers [8,16]. The values of ΔG^{o}_{ads} are approximately ranged from –39 to –41 kJ mol^{-1} at 298 K and from –38 to –40 kJ mol^{-1} at 323 K. It is well established that values of ΔG^{o}_{ads} up to –20 kJ mol^{-1} are consistent with the electrostatic interaction between the charged molecules and the charged metal (physisorption), while the values that involve charge sharing or charge transfer from the inhibitor molecules to the metal surface to form a co-ordinate type of bond (chemisorption) are –40 kJ mol^{-1} or more negative [10,12].

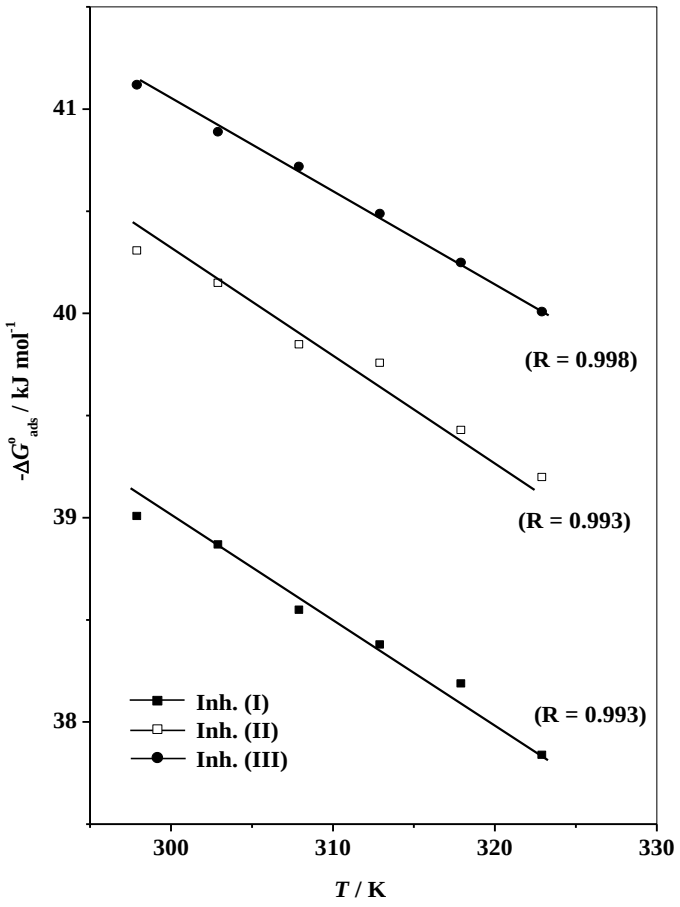

Figure 5. Effect of temperature on the free energy of adsorption (ΔG^{o}_{ads}) for TDADs (I–III) on 1018 carbon steel in 0.5 M NaCl solution.

The calculated ΔG^{o}_{ads} values of TDADs in neutral chloride solution indicate, therefore, that the adsorption mechanism of these compounds on 1018 carbon steel surface involves two types of interaction, chemisorption and physisorption. Indeed, due to the strong adsorption of water molecules on carbon steel surface, one may assume that adsorption occurs first due to the physical force. The removal of water molecules from the surface is accompanied by chemical interaction between the metal surface and the adsorbate that turns to chemisorptions [12]. The K_{ads} values follow the same trend in the sense that large values of K_{ads} imply more efficient adsorption and hence better protection effectiveness.

Table 2. Thermodynamic parameters of the adsorption of TDAD inhibitors (I–III) on 1018 carbon steel surface in 0.5 M NaCl solutions at different temperatures

Inhibitor	T (K)	10^{-4} K_{ads} (mol^{-1})	$-\Delta G^{o}_{ads}$ (kJ mol^{-1})	$-\Delta H^{o}_{ads}$ (kJ mol^{-1})	$-\Delta S^{o}_{ads}$ (J mol^{-1} K^{-1})
I	298	12.4	39.0	52.8	46.1
	303	9.0	38.9		
	308	6.2	38.5		
	313	4.6	38.4		
	318	3.4	38.2		
	323	2.4	37.8		
II	298	20.9	40.3	53.6	44.6
	303	15.0	40.1		
	308	10.3	39.8		
	313	7.8	39.6		
	318	5.4	39.4		
	323	3.9	39.2		
III	298	28.5	41.1	53.8	42.6
	303	20.0	40.9		
	308	14.5	40.7		
	313	10.3	40.5		
	318	7.3	40.2		
	323	5.3	40.0		

The negative value of ΔH^{o}_{ads} indicates that the adsorption of TDADs (I–III) molecules on carbon steel surface is an exothermic process. This agrees with the decrease in the values of η_i% with rise of temperature, as shown in Table 3. Such behavior can be interpreted on the basis that increase in temperature resulted in desorption of some adsorbed inhibitor molecules from the surface [16]. A conclusion which is further confirmed from the observed limited decrease in the absolute value of ΔG^{o}_{ads} with increase in temperature (Table 2), indicating that adsorption is somewhat unfavorable with rise in temperature and that physisorption has the major contribution while chemisorption has the minor contribution in the adsorption mechanism [31].

Table 3. Effect of temperature on η_i% of 1018 carbon steel corrosion in 0.5 M NaCl solution in the presence of 11 μM of TDADs (I–III)

T (K)	η_i%		
	I	II	III
298	58	77	79
303	58	72	77
308	57	66	71
313	55	59	66
318	54	56	62
323	53	54	56

3.2.3. Activation parameters

The effect of temperature on the corrosion rate of 1018 carbon steel in 0.5 M NaCl solution free or containing 11 μM from TDADs I, II or III over the range 298 – 323 K was also investigated. From the results of η_i% obtained as a function of temperatures (Table 3), one can conclude that as the temperature increases the η_i% decreases for all compounds used, due to increase in corrosion rate through thermal activation of the dissolution reaction at higher temperature.

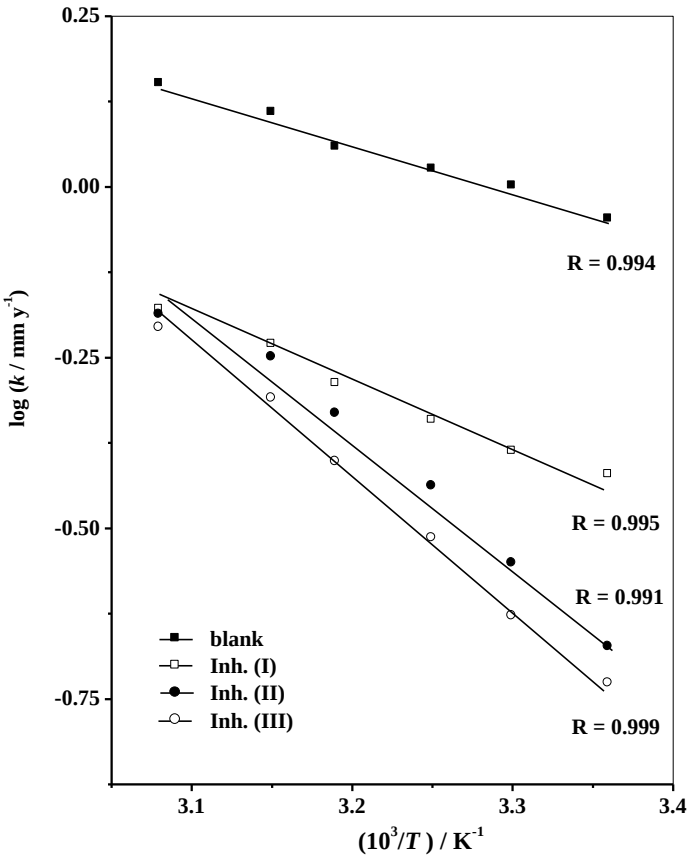

Figure 6. log *k* – 1/*T* plots for 1018 carbon steel dissolution in 0.5 M NaCl solution in the absence and presence of 11 μM of TDADs (I–III).

The apparent activation energy (E_a^*) of the corrosion process was calculated from Arrhenius plots of log k vs. $1/T$ for carbon steel in 0.5 M NaCl solution in the absence and presence of 11 μM of inhibitors (I–III) as shown graphically in Fig. 6 using the following equation:

$$\log k = A - (E_a^*/2.303RT) \quad (7)$$

where A is the Arrhenius pre-exponential factor which depends on the metal type and electrolyte. The plots are all linear relationships and the values of E_a^* obtained from their slopes are presented in Table 4. The results reveal that E_a^* increases in the same order of increasing protection efficiency of TDADs used, which confirms that compound III exhibits the best performance even at temperature as high as 323 K. It is also obvious that the whole corrosion process is controlled by surface reaction, since the activation energy of the corrosion process is over 20 kJ mol^{-1} [22]. The high value of E_a^* is a good support for the strong adsorption of TDAD on the steel surface, suggesting that the adsorbed TDAD act as a negative electrocatalyst for the corrosion process of 1018 carbon steel by blocking the active sites for metal dissolution on the sample surface, thus creating an energy barrier for mass and charge transfer, leading to a decrease in the corrosion current density commensurate with an increase in the polarization resistance (R_p) of the electron transfer.

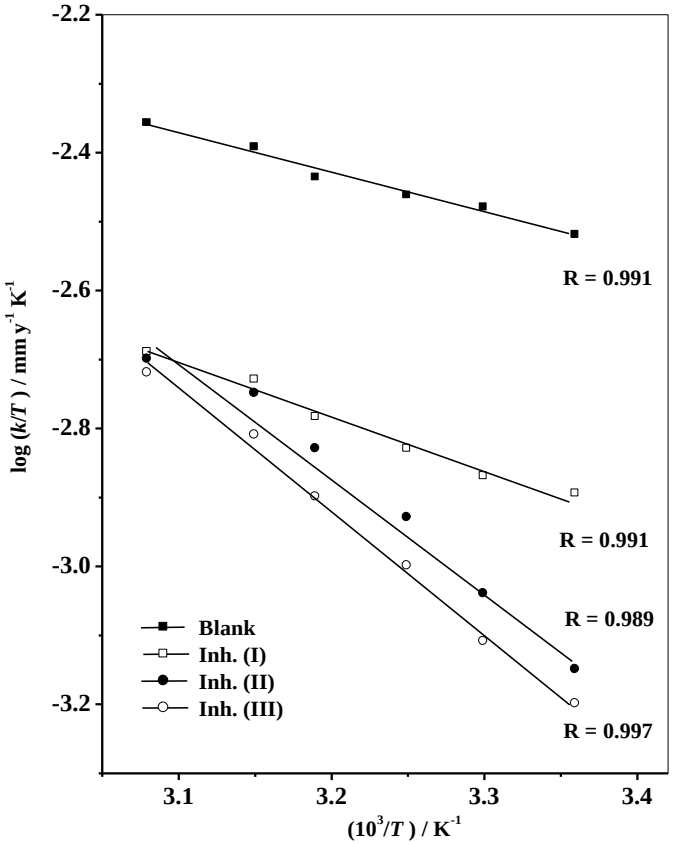

Figure 7. log (k/T) – ($1/T$) plots for 1018 carbon steel dissolution in 0.5 M NaCl solution in the absence and presence of 11 μM of TDADs (I–III).

Enthalpy and entropy of activation (ΔH^*, ΔS^*) are calculated from the transition state theory using the following equation [16,24]:

$$k = \frac{RT}{Nh}\ exp(\frac{\Delta S^*}{R})\ \ exp(\ \frac{-\Delta H^*}{RT}) \qquad (8)$$

where h is the Planck's constant and N is the Avogadro's number. Plots of log k/T vs. $1/T$ (Equation 8) for carbon steel dissolution in chloride solution free or containing 11 μM from compound I, II or III are all linear as shown in Fig. 7. From the slopes ($-\Delta H^*/2.303R$) and the intercepts (log RT/Nh + ($\Delta S^*/2.303R$)) of these plots, values of ΔH^* and ΔS^* for the corrosion process were calculated and listed in Table 4.

Table 4. Activation parameters for the corrosion process of 1018 carbon steel in 0.5 M NaCl solution in the absence and presence of 11 μM of TDAD inhibitors (I–III)

Blank	13.5	11.0	256.6
I	17.3	14.9	250.9
II	34.1	32.1	197.2
III	36.1	34.0	192.3

As can be seen, in the presence of TDADs, the trend for the increase in ΔH^* value is mirrored completely by that for the apparent activation energy (E_a^*). Furthermore, the negative large values of ΔS^* in the absence and presence of the tested compounds indicate that activated complex in the rate-determining step represents an association rather than dissociation step, meaning that increasing in the system order takes place on going from reactants to the activated complex, where the activated molecules are in more ordered state than at the initial one [16,32]. The degree of corrosion protection of 1018 carbon steel by the investigated compounds as gathered from the increase in E^*_a and ΔH^* and the decrease in ΔS^* values remains unchanged and follows the sequence: III > II > I.

3.3. Pitting corrosion inhibition

Breakdown of the passivating film on a metal by aggressive anions like chloride and other halides, and sometimes sulfide, occurs locally rather than generally. Microanodes of active metals are surrounded by large cathodic protective areas of the passive metal. This fixes the position of anode and results in pitting corrosion. Pitting corrosion of carbon steel is of great practical interest, it can be a destructive form of corrosion in engineering structures if it causes perforation of equipment causing its failure. Therefore, the effect of adding different concentrations of TDADs (I–III) on the breakdown potential for the initiation and propagation of pitting corrosion of anodized 1018 carbon steel in 0.5 M

NaCl solution was investigated. After the corrosion potential, the anodic current density starts to increase in the active region due to iron dissolution ($Fe \rightarrow Fe^{2+}+2e^{-}$). Figure 8 and similar ones, all show that the forgoing anodic scans of carbon steel in the presence of TDADs characterize by potential domain of passivition (~400 mV). Upon increasing the potential beyond the passive region, the small passive current density rises rapidly and steeply without any sign for oxygen evolution, indicating initiation of pitting corrosion when the polarization potential reaches a certain critical value (E_{pit}). Once a pit is nucleated, pitting growth and propagation is proceeded via an active dissolution mode leading to breakdown of the passivating film at higher anodic potential. Figure 9 shows the relationship between E_{pit} and the logarithm of inhibitor concentration for the three derivatives, where linear plots are obtained in fitting to the following equation:

$$E_{pit} = a - b \log C \quad (9)$$

where a and b are two empirical constants depending on the corroding system. The plots show that pitting corrosion of carbon steel depends on both inhibitor nature and its concentration.

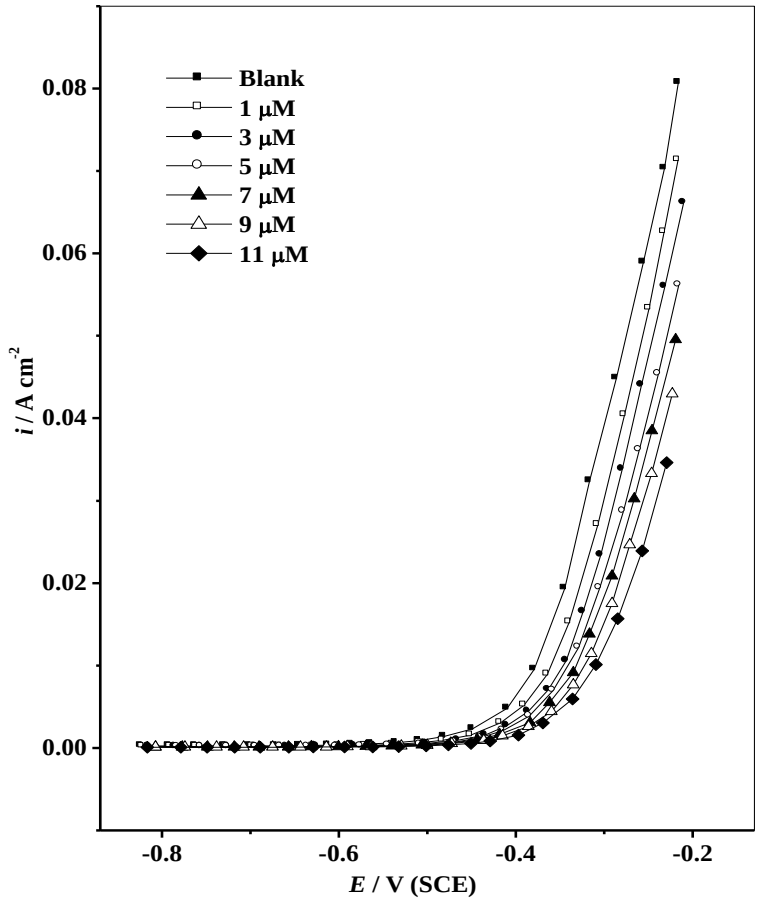

Figure 8. Potentiodynamic anodic polarization scans for 1018 carbon steel dissolution in 0.5 M NaCl solution in the absence and presence of different concentrations of inhibitor (III) at 298 K.

Table 5. Pitting potentials of 1018 carbon steel in 0.5 M NaCl solution in the presence of different concentrations of compounds (I–III) at 298 K

	I	II	III
1	390	385	382
3	373	368	365
5	367	361	358
7	359	355	349
9	350	347	344
11	347	342	338

E_{pit} for the blank = –391 mV(SCE)

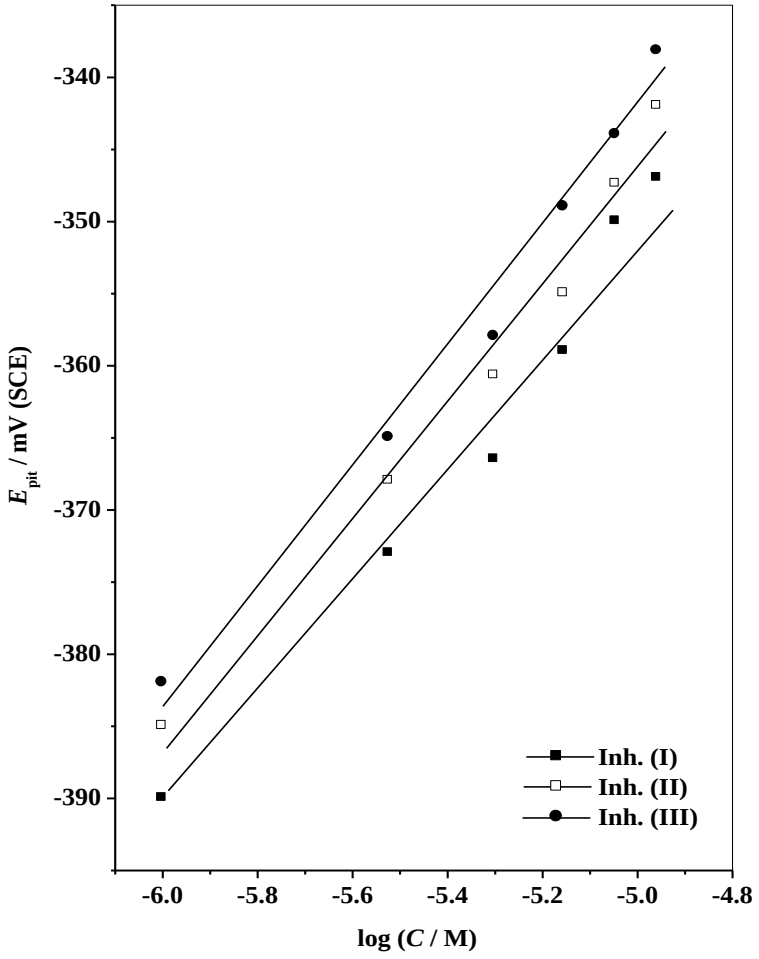

Figure 9. Pitting potential (E_{pit}) as a function of TDADs (I–III) concentrations for 1018 carbon steel in 0.5 M NaCl solution at 298 K.

Table 5 indicates that increase in inhibitor concentration shifts the value of E_{pit} to more positive potentials commensurate with an increase in the alloy resistance to passivity breakdown. The mitigation influence of TDADs (I–III) is likely attributed to the formation of surface adsorbed layer, which preclude the aggressive anion from reaching to the base carbon steel surface and thereby hinder pit initiation. This effect decreases in the order III > II > I, which is the same sequence for the decrease in the corrosion rate or the increase in the effectiveness of these compounds to protect the metallic substrate.

The aggressiveness of halide ions as a pitting agent is attributed to their competitive adsorption on the film surface [33]. At E_{pit}, the initiation of pitting attack at high anodic potential could be ascribed to competitive adsorption between Cl^- ions and the passive species (OH^- and H_2O dipoles). The Cl^- anions displace the adsorbed passivating species at some locations and accelerate localized anodic dissolution. On the other hand, the initiation of pitting attack could be due to the ability of Cl^- anions to penetrate the passive film with the assistance of a high electric field across this film and to attack the base metal surface [34].

3.4. Electrochemical Impedance Spectroscopy

The results of potentiodynamic polarization experiments were confirmed by electrochemical impedance spectroscopy (EIS), which is a powerful technique in accurately predicting and control the corrosion behavior of metallic materials [35]. The experimental impedance results are simulated to pure electronic models that can verify or role out mechanistic models and enable the calculation of numerical values corresponding to the physical and/or chemical properties of the electrochemical system under investigation [24,36]. The role of TDADs with various concentrations on the corrosion behavior of 1018 carbon steel in 0.5 M NaCl solution was investigated at 298 K. The experimental EIS data were recorded over the frequency range from 100 kHz to 1 Hz at OCP after 30 min of immersion in solutions without and with addition of various concentrations of compounds (I–III). Fig. 10a, b displayed the obtained impedance response as Bode and Nyquist plots for compound III. As can be seen, log |Z| in Fig. 10a tends to become of a typical resistive behavior at high and low frequencies, with phase angle (ϕ) values falling towards zero degree, while at intermediate frequencies the behavior of log |Z| becomes capacitative and the phase angle acquires a maximum value (ϕ_{max}). On the other, Nyquist diagrams in Fig. 10b consist from only one large capacitive loop considerably increases in the presence of TDAD, in consistent with the increase in log |Z| and ϕ_{max} values of the Bode diagram compared to their values in the blank chloride solution.

The corrosion of carbon steel is an example of simple charge transfer process [16]. Thus, by using a constant phase element (CPE), the simple Randles equivalent circuit depicted as an inset in Fig. 10b was found to be adequate for fitting the impedance data [19,37]. The model consists of a solution resistance (R_s) in series with RC parallel combination of (R_t/Q_{dl}), which represents the charge transfer resistance and a constant phase element instead of an ideal capacitance element for the double layer, respectively. In case of solid materials, the usage of CPE is to describe the non-homogeneities in the system [38]. The R_t values refer to charge transfer resistance of the steel/electrolyte interface and the

TDAD adsorbed film resistance. The high frequency limits of this model correspond to R_s, while the low frequency limits show the kinetic response of the charge transfer resistance and the solution resistance (R_t + R_s) [37]. The CPE is described by the expression: $Z_Q = [Q(j\omega)^{\alpha}]^{-1}$. Where Q is the frequency independent constant, j^2 is -1, ω is the angular frequency and α value is the correlation coefficient for the CPE ($0 < \alpha < 1$). Accordingly, Q is identical to C_{dl} at ω = 1 [12,39,40].

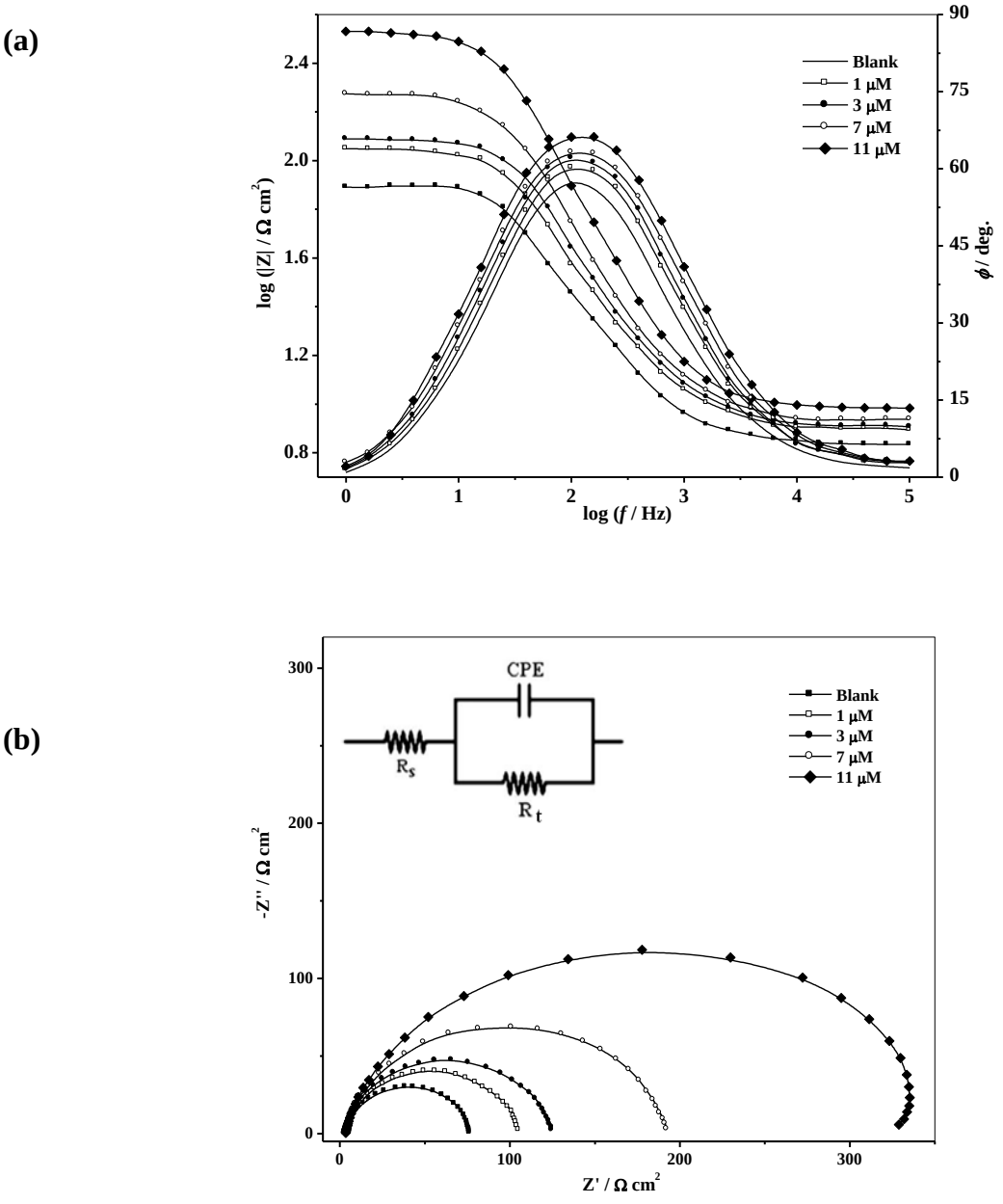

Figure 10. Bode (a) and Nyquist (b) impedance plots for 1018 carbon steel dissolution in 0.5 M NaCl solution in the absence and presence of different concentrations of TDAD (III) at 298 K. The insert in Fig. 10b represents the Randles model with a constant phase element (CPE) used to fit the experimental EIS data.

The main impedance parameters obtained for 1018 carbon steel in 0.5 M NaCl solution as a function of TDADs (I–III) concentrations are listed in Table 6 together with the surface coverage (θ) and the protection efficiency (η_{Rt}%) derived from the impedance charge transfer according to Eq. 3. As can be seen, addition of TDADs increases the values of R_t and reduces the C_{dl}. The increase in R_t values, and consequently in the inhibition efficiency, is attributed to the formation of a protective film on the metal/solution interface [12,41]. This protective film is formed by gradual replacement of water molecules with adsorbed inhibitor molecules, leading to an increase in the thickness of the electronic double layer and a decrease in its electrical capacitance (C_{dl}) [12,24]. Also, the decrease in C_{dl} can result from a decrease in local dielectric constant, which suggests that TDAD molecules functions by adsorption [10,42].

Table 6. Electrochemical impedance parameters for 1018 carbon steel in 0.5 M NaCl solution in the absence and presence of different concentrations of TDADs (I–III) at 298 K

Blank	0	75	41.25	57.5	-----	-----
I	1	84	38.21	59.6	0.11	11
	3	100	38.02	61.2	0.25	25
	7	134	36.53	62.5	0.42	42
	11	187	34.59	65.1	0.59	59
II	1	96	37.95	59.7	0.22	22
	3	120	37.82	61.3	0.36	36
	7	158	36.22	62.7	0.53	53
	11	295	35.04	65.6	0.75	75
III	1	101	37.21	60.2	0.26	26
	3	122	37.15	61.5	0.39	39
	7	187	36.50	63.2	0.60	60
	11	332	34.02	66.5	0.77	77

The inhibition efficiencies calculated from EIS results (η_{Rt}%) show the same trend as those obtained from polarization measurements (η_i%). The difference in the efficiencies from the two methods may be attributed to different surface status of the electrode in the two measurements. EIS measurements were performed at the rest potential, while in polarization measurements the electrode potential was polarized to high overpotential, non-uniform current distributions resulted from cell geometry, solution conductivity, counter and reference electrode placement, etc., will lead to difference between the electrode area actually undergoing polarization and the total area [43].

Referring to the values of ϕ_{max} given in Table 6, it is well known that the maximum phase angle (ϕ_{max}) should be 90° for a corroding system represented by a simple *RC* parallel combination when *R*s = 0. However, depressed semicircles are usually obtained for a practical electrode/solution interface,

which has been known to be associated with a rough electrode surface [22]. Corrosion of carbon steel in NaCl solution increases the roughness of the electrode surface and therefore reduces the value of ϕ_{max}, amounting to 57.5–66.5°. Additionally, a less depressed semicircle with higher ϕ_{max} indicates a better quality of the inhibitor monolayer.

3.5. SEM micrography

The surface morphologies of grade 1018 carbon steel specimen in 0.5 M NaCl solution free or containing 11 μM TDADs (I–III) after 2 h immersion were examined using SEM as displayed in Fig. 11(a–d), respectively. In the absence of inhibitors (Fig. 11a), a very rough surface is observed due to rapid corrosion attack of carbon steel by chloride anions. There are a large number of pits surrounded by iron oxide layer which almost fully covers the carbon steel surface, revealing that pit formation under these conditions occurs continuously during the exposure period while iron oxide builds up over the surface [44]. It is important to stress out that when TDADs (I–III) are present in the solution, the morphology of carbon steel surface are quite different from the previous one and the rough surface (the amount of formed iron oxide and the number of pits) is visibly reduced in the order I > II > III, indicating the formation of a protective film with inhibiting power that increases in the reverse order. These conspicuous variations in the microstructures of the films reflect the same trend of the inhibitive properties of the added compounds as obtained from the electrochemical measurements.

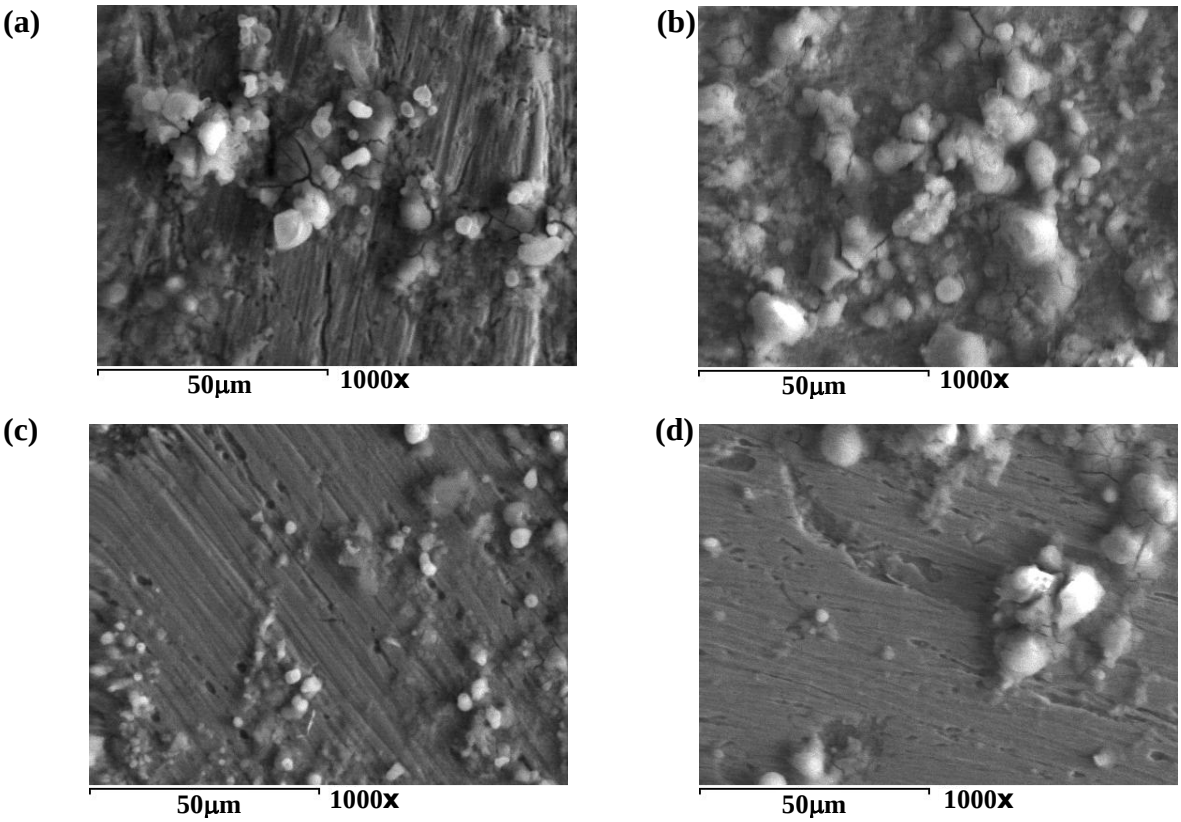

Figure 11. SEM morphologies for 1018 carbon steel surface after 2 h immersion in 0.5 M NaCl solutions in the absence (a) and presence of 11 μM of TDAD I (b), II (c) and III (d).

4. CORROSION PROTECTION MECHANISM

Under neutral conditions, the major reaction governing corrosion in most practical applications is the reduction of oxygen present in solution. In pure dry air at normal temperature a thin protective oxide film forms on carbon steel surface. Unlike that formed on stainless steels, it is not protective in the presence of electrolytes and it is usually breakdown and dissolves [45]. The obtained results from various electrochemical techniques indicate that the investigated new TDADs can protect carbon steel from corrosion in chloride solution on the basis of molecular adsorption. The adsorbility of these molecules depends mainly on certain physicochemical properties of the inhibitor molecules such as functional groups of the donor atom and π orbital character of donating electrons, as well as the electronic structure of the molecules [46].

Generally, the adsorption of organic compounds can be described by two main modes of interaction: physisorption and chemisorption. The former requires the presence of electrically charged metal surface and charged species in the bulk of solution, while the latter involves charge-sharing or charge-transfer from the inhibitor molecules to the metal surface to form a co-ordinate type of a bond. This is possible in case of a positive as well as negative charge on the surface [47]. It is worth noting that a combination of both processes is possible [12], in consistent with the values of thermodynamic adsorption functions (ΔG^{o}_{ads}, ΔH^{o}_{ads}) obtained here (Table 2). A representation for the proposed adsorption model of the investigated TDADs molecules is depicted in Fig. 12. This model clearly indicates the active adsorption centers which are the electronegative hetero-atoms N, O and S, in addition to π-electrons on aromatic nuclei. Efficient adsorption occurs with one of these atoms or through π-electrons of the aromatic ring or both of them.

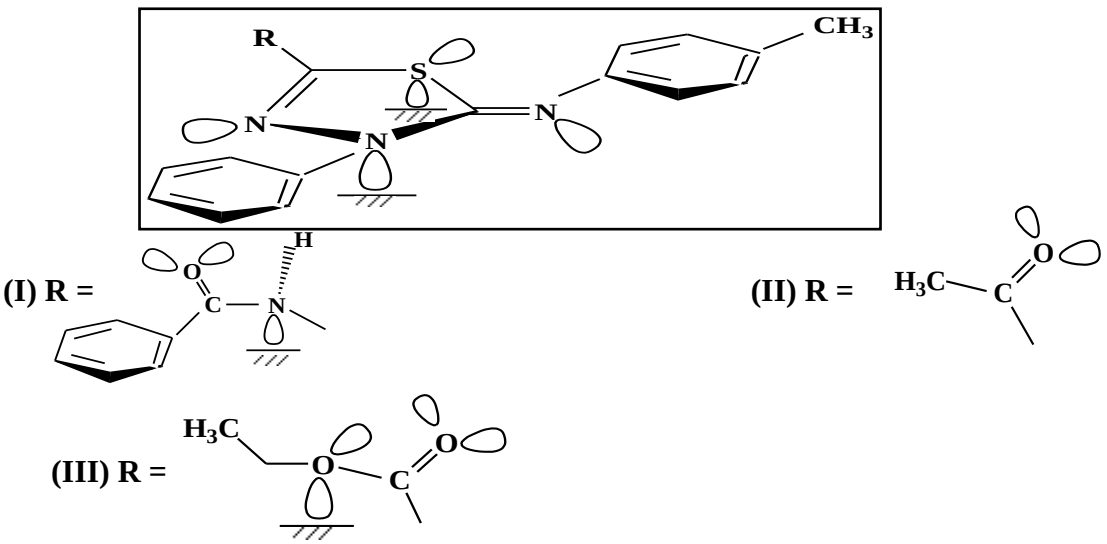

Figure 12. A representation for the proposed adsorption model of TDADs (I–III) on 1018 carbon steel surface.

It was observed during the experiments that the free corrosion potential of carbon steel in 0.5 M NaCl solution without inhibitor is –712 mV(SCE), and the previously determined [48] value for the potential of zero charge ($E_{q=0}$) in chloride-containing solution of pH 6 is –725 mV(SCE). This means that the charge on a correlative scale: $\varphi_c = E_{corr} - E_{q=0}$, for carbon steel surface is positive. Therefore, adsorption of TDADs molecules on anodic sites occurs through the formation of an iron-nitrogen co-ordination bond and by a π-electrons interaction between the π-electrons in the aromatic ring of the inhibitor and the vacant d-orbitals of iron surface, leading to decrease the anodic dissolution of carbon steel [32].

The extent of protection for the three investigated TDADs is in the order: III > II > I. Compound III is more efficient than compound II due to its higher molecular size. It follows that the ethoxy group is more efficient than the methyl one. From structural organic point of view, both methyl and ethoxy groups have +R effect but the inductive effect is +I for methyl group and –I for ethoxy group, although the methyl group has +R but its effect is very little as a result of hyperconjugation. In the case of ethoxy group both the effects of +R and –I are larger. Moreover, ethoxy group may add an additional active center to compound (III) and this increases the inhibition efficiency of compound (III) than compound (II). Compound (I) is the least efficient inhibitor in spite of its larger molecular size compared to the others and it has the same number of adsorption active centers. This can be explained on the basis of the absence of a conjugation between the carbonyl group (–C=O) with azomethine (–N=C–) group in the thiadiazole ring of compounds (I). This leads to lesser surface coverage by compound (I) and thereby, gives lower protection efficiency than the other tested compounds (II and III). This conclusion is further confirmed by calculating the values of the highest occupied (HOMO) and the lowest unoccupied (LUMO) molecular orbital energies [49] with Gauissian 98 software package for PC, using the drawing program Hyperchem and optimization to be more stable with PM3. The values obtained for derivatives I, II and III, respectively are: $-E_{HOMO}$ = 3.5807, 3.4807 and 3.3763 eV and E_{LUMO} = 7.8341, 7.8424 and 8.000 eV. The decrease in the absolute E_{HOMO} (i.e. with decreasing ionization potential) and the increase in E_{LUMO} or the electron affinity is in an order which runs parallel to the increase in the protection efficiency, indicating that TDAD (III) is the most efficient inhibitor among the studied three compounds.

5. CONCLUSIONS

1. Corrosion protection of carbon steel in 0.5 M NaCl solution was investigated by testing the inhibition performance of new thiadiazole derivatives (I–III) using electrochemical techniques.

2. The protection power η_i% or η_{Rt}% increases with increase in inhibitor concentration, and at any given conditions it decreases in the order: III > II > I. The charge transfer resistance (R_t) follows the same trend, and this is confirmed by surface examination.

3. The three tested compounds were found to be anodic-type inhibitors, i.e. they affect anodic dissolution reaction of carbon steel by blocking the active anodic sites on the metal surface.

4. The protection afforded by TDADs (I–III) is due to the adsorption of their molecules on carbon steel surface. The adsorption behavior follows Langmuir adsorption isotherm.

5. Thermodynamic adsorption functions corroborate a combination of spontaneous physisorption and chemisorption modes of interactions between the inhibitor molecules and the metallic substrate.

6. The adsorbed layer creates a barrier for mass and charge transfers that can protect carbon steel against general and pitting corrosion in neutral chloride solution.

References

1. F.M. Al-Kharafi, B.G. Atea and R.M. Abd Alla, *J. Appl. Electrochem.* 32 (2002) 1363.
2. K. Aramaki and T. Shinura, *Corros. Sci.* 48 (2006) 209.
3. J.R. Galvele, *Corros. Sci.* 21 (1981) 551.
4. L. Garverik (Ed.), *Corrosion in Petroleum Operations, in: Corrosion in the Petrochemical Industry,*
5. Metal Park, ASM International, OH (1994).
6. M. Mahdavian and S.A. Ashhari, *Electrochim. Acta,* 55 (2010) 1720.
7. L. Valek and S. Martinez, *Mater. Lett.* 61 (2007) 148.
8. M.E. Azhar, B. Mernari, M. Traisnel, F. Bentiss and M. Lagrenée, *Corros. Sci.* 43 (2001) 2229.
9. M. Lebrini, M. Lagrenée, H. Vezin, M. Traisnel and F. Bentiss, *Corros. Sci.* 49 (2007) 2254.
10. M. Lebrini, F. Bentiss, H. Vezin and M. Lagrenée, *Corros. Sci.* 48 (2006) 1279.
11. M. Lebrini, M. Lagrenée, M. Traisnel, L. Gengembre, H. Vezin and F. Bentiss, *Appl. Surf. Sci.* 253 (2007) 9267.
12. F. Bentiss, M. Lebrini, M. Lagrenée, M. Traisnel, A. Elfarouk and H. Vezin, *Electrochim. Acta*, 52 (2007) 6865.
13. Y. Tang, X. Yang, W. Yang, Y. Chen and R. Wan, *Corros. Sci*. 52 (2010) 242.
14. I.L. Rozenfeld, *Corrosion Inhibitors*, McGraw-Hill Inc., New York (1981).
15. J.G.M. Thomas, in: L.L. Shrier, R.A. Jarman and G.T. Burstein (Eds), Corrosion, third ed., Butterworth-Heinemann, Oxford (1994).
16. P. Morales-Gil, G. Negron-Silva, M. Romero-Romo, C. Angeles-Chávez and M. Palomar-Pardavé, *Electrochim. Acta,* 49 (2004) 4733.
17. A.S. Fouda, F. El-Taib Heakal and M.S. Radwan, *J. Appl. Electrochem*. 39 (2009) 391.
18. M. Lebrini, M. Traisnel, M. Lagrenée, B. Mernari and F. Bentiss, *Corros. Sci*. 50 (2008) 473.
19. A.O. Abd El-Hamid, B.A.M. Abd El-Wahab and A.A. Al-Atom, *Phosphorus Sulfur Silicon Relat. Elem*. 179 (2004) 601.
20. F. El-Taib Heakal and S. Haruyama, *Corros. Sci*. 20 (1980) 887.
21. C.B. Shen, S.G. Wang, H.Y. Yang, K. Lang and F.H. Wang, *Electrochim. Acta,* 52 (2007) 3950.
22. S.S. El-Egamy, *Corros. Sci*. 50 (2008) 928.
23. S.S. Abd El-Rehim, O.A. Hazzazi, M.A. Amin and K.F. Khaled, *Corros. Sci*. 50 (2008) 2258.
24. A.M. Shams El-Din, R.A. Mohammed and H.H. Haggag, *Desalination* 114 (1997) 85.
25. F. El-Taib Heakal and A.M. Fekry, *J. Electrochem. Soc*. 155 (2008) C543.
26. M.A. Amin, K.F. Khaled and S.A. Fadl-Allah, *Corros. Sci*. 52 (2010) 140.
27. A.K. Mohamed, H.A. Mostafa, G.Y. El-Awady and A.S. Fouda, *Port. Electrochim. Acta*, 18 (2000) 99.
28. S.A. Ali, H.A. Al-Muallem, M.T. Saeed and S.U. Rahman, *Corros. Sci*. 50 (2008) 664.
29. N.K. Allam, *Appl. Surf. Sci*. 253 (2007) 4570.
30. S.T. Hirozawa, *Proceeding of 8th European symposium on corrosion inhibitors,* vol 1, Ann University, Ferrara, Italy (1995) p. 25.
31. X.H. Li, S.D. Deng, H. Fu and G.N. Mu, *J. Appl. Electrochem*. 39 (2009) 1125.
32. M.G. Hosseini, H. Khalidpur and S. Ershad, *J. Appl. Electrochem*. 40 (2010) 215
33. S.K. Shukla and M.A. Quraishi, *J. Appl. Electrochem*. 39 (2009) 1517.

34. S.A.M. Refaey, F. Taha and A.M. Abd El-Malak, *Appl. Surf. Sci*. 242 (2005) 114.
35. D.C.W. Kannagara and B.E. Conway, *J. Electrochem. Soc*. 134 (1987) 894.
36. J.R. Macdonald, *Impedance Spectroscopy*, John Wiely & Sons, New York (1987).
37. F. El-Taib Heakal, A.M. Fekry and M.Z. Fatayerji, *J. Appl. Electrochem*. 39 (2009) 1633.
38. F. Mansfeld, *Electrochim. Acta*, 35 (1990) 1533.
39. F. Mansfeld, M.W. Kendig and S. Tsai, *Corrosion*, 38 (1982) 570.
40. D. Marijan and M. Gojic, *J. Appl. Electrochem*. 32 (2002) 1341.
41. F. El-Taib Heakal, A.A. Ghoneim and A.M. Fekry, *J. Appl. Electrochem*. 37 (2007) 405.
42. S.K. Shukla and M.A. Quraishi, *Corros. Sci*. 52 (2010) 314.
43. E. McCafferty and N. Hackerman, *J. Electrochem. Soc*. 119 (1972) 146.
44. R.G. Kelly, J.R. Scully, D.W. Shoesmith and R.G. Buchheit, *Electrochemical Techniques, in: Corrosion Science and Engineering*, Marcel Dekker Inc., New York (2002) p. 148.
45. L. Caceres, T. Vargas and L. Herrera, *Corros. Sci*. 51 (2009) 971.
46. Y.F. Chen, M. Wilmott and J.L. Luo, *Appl. Surf. Sci.* 152 (1999) 161.
47. C.B. Shen, S.G. Wang, H.Y. Yang, K. Long and F.H. Wang, *Electrochim. Acta*, 52 (2007) 3950.
48. M. Lebrini, M. Lagrenée, H. Vezin, L. Gengembre and F. Bentiss, *Corros. Sci*. 47 (2005) 485.
49. M.A. Amin, S.S. Abd El-Rehim, E.E.F.El-Sherbini and R.S. Bayoumi, *Electrochim. Acta*, 52 (2007) 3588.
50. M. Behpour, S.M. Ghoreishi, N. Soltani, M. Salavati-Niasari, M. Hamadanian and A. Gandomi, *Corros. Sci*. 50 (2008) 2172.